We are IntechOpen,
the world's leading publisher of
Open Access books
Built by scientists, for scientists

5,800
Open access books available

142,000
International authors and editors

180M
Downloads

154
Countries delivered to

Our authors are among the

TOP 1%
most cited scientists

12.2%
Contributors from top 500 universities

CLARIVATE ANALYTICS

BOOK CITATION INDEX

INDEXED

WEB OF SCIENCE™

Selection of our books indexed in the Book Citation Index
in Web of Science™ Core Collection (BKCI)

Interested in publishing with us?
Contact book.department@intechopen.com

Numbers displayed above are based on latest data collected.
For more information visit www.intechopen.com

Chapter

Fluoride Detection and Quantification, an Overview from Traditional to Innovative Material-Based Methods

Eugenio Hernan Otal, Manuela Leticia Kim and Mutsumi Kimura

Abstract

Fluorine is the 13th most abundant element on Earth, and fluoride is part of our everyday lives, present in our drinking water, beauty products, and naturally present in food and beverages. It is a key element to increase the resistance of the dental enamel to the acidic bacteria attack and prevent dental decay. However, the ingestion of this anion for an extended period of time and in concentrations over the recommended limits can produce mild to severe health issues, called fluorosis, that can produce incorrect dental enamel formation, reduce the functionality of joints and even affect the bone structure. To avoid these terrible effects, it is necessary to control the fluoride levels in drinkable water, particularly in communities without access to safe water networks. To achieve this goal, the first step is to identify safe water sources and provision portable and reliable sensors to these communities. A major step towards safe water accessibility would be the implementation of these sensors by the proper use of new materials and technologies. Here we present an overview of the traditional quantification methodologies and the new ones for fluoride detection and quantification, and the future trends on portable devices for user-friendly on-point measurements.

Keywords: fluorides, fluorosis, sensors, metal–organic frameworks, portable devices, smartphones

1. Introduction

Fluoride is the inorganic anion of Fluorine. As all the halogens in -1 state, it generates colorless salts and can be classified as a weak base due to the $pK_a^{\mathrm{HF}} = 3.2$. Fluorine is in the 13th position of abundance in the earth, and it is present only in the anion form as fluorite (CaF_2), the most abundant fluoride mineral.

The most relevant use for fluoride is cavity prevention, due to the presence of fluoride in water, toothpaste, and fluoride therapy in the form of sodium fluoride (NaF) or sodium monofluorophosphate (Na_2PO_4F). Water fluoridation is considered by the U.S. Centers for Disease Control and Prevention (CDC) as *"one of 10 great public health achievements of the twentieth century"* [1].

Fluoride is present in dental products, food, and drinking water. Fluoride content in dental products is between 1.0 and 1.5 mg kg^{-1}. Vegetables and fruits have a low content (0.1–0.4 mg kg^{-1}), while rice and barley can contain higher fluoride levels (2 mg kg^{-1}). Meat and fish can have higher concentrations, but it is accumulated in bones, which does not represent a risk. The dietary recommendations for adults in U.S.A. are between 3.0 and 4.0 mag day^{-1}, while in Europe are between 2.9 and 3.4 mag day^{-1}. The major known risk of fluoride deficiency is the risk of tooth cavities.

On the other hand, excess fluoride can conduce to health problems. World Health Organization (WHO) settled the recommended upper limit for fluoride in drinking water to 1.5 mg kg^{-1} [2]. Prolonged exposure to higher levels of fluorides above the recommended limit can cause dental fluorosis (1.5–3 mg kg^{-1}), which exhibits defects in enamel formation, mottling, browning, and severe teeth deterioration. Higher concentrations (4–8 mg kg^{-1}) can cause skeletal fluorosis, where the bones are hardened and less elastic, increasing the frequency of fractures. Even higher concentrations can cause crippling deformities of the spine and major joints, reducing body mobility and can also cause neurological defects and compression of the spinal cord.

The incidence of fluorosis is low in urban populations but more frequent in rural populations. The most affected areas are located in the south of South America, Southwest North America, north and east coast of Africa, India, and China [3]. In the case of east coast of Africa, fluoride concentration is related to geological formation, like volcanic activity, (East African Rift through Sudan, United Republic of Tanzania, Uganda, Ethiopia, and Kenya). Kenyan Lakes of Najura and Elmentaita presented 2800 and 1630 mg kg^{-1} fluoride, respectively, and Tanzanian Momella soda lakes presented 690 mg kg^{-1} fluoride.

As the contamination of natural waters with fluoride are mainly geogenic than anthropogenic, and thus the distribution of fluorides levels is determined by the geological formation of the riverbeds. This scenario generates an inhomogeneous distribution of fluoride levels in the water sources, even in small areas. In **Figure 1**, the distribution of fluoride levels in Arusha, Tanzania is shown. The red spots represent water sources with fluoride concentration above WHO recommendations and the blue ones below this level. The figure shows that safe and unsafe water sources can be closed and with adequate information, the local populations can choose the safer water source and avoid health risks [4].

Recently, the water fluoridation effectiveness against teeth decay was strongly questioned [5]. Countries without water fluoridation systems, like Denmark, exhibit tooth decay rates similar to US communities with fluoridation. This observation makes it necessary to rethink the need for water fluoridation to prevent cavity prevention. The amount of fluorides in toothpaste and rinses seems to be enough to protect the teeth enamel. When fluoride ions are in the mouth, they are incorporated into plaque. When the pH decreases, the fluoride ions are released from the plaque and participate in the remineralization process, which slows down the tooth decay rate. The fact that the cells involved in the remineralization process, the ameloblasts, are affected by the presence of fluorides, suggests that other cells in the body can also be affected. The relationship
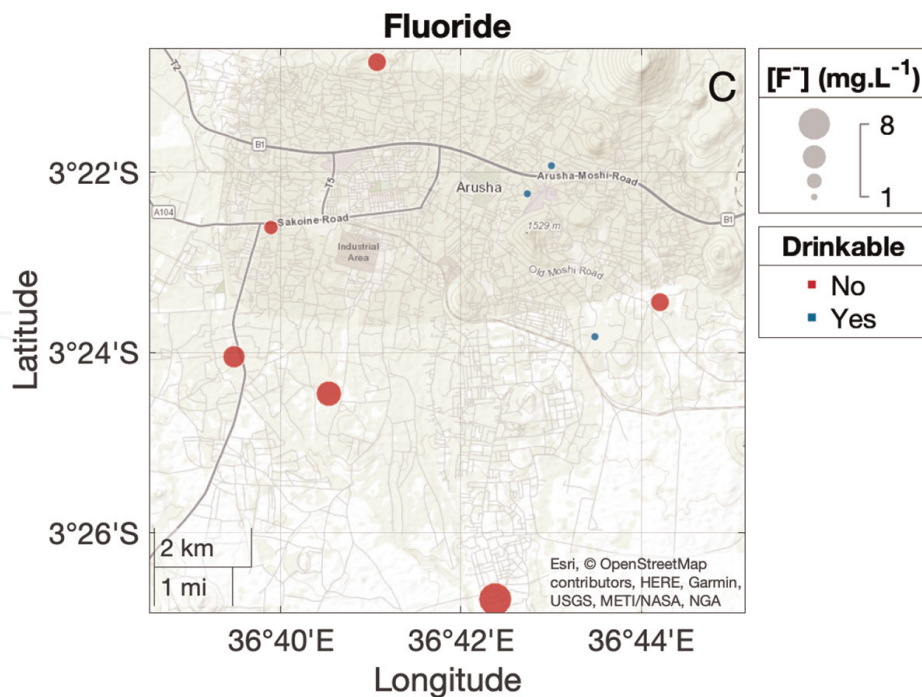
Figure 1.
Distribution of fluoride on different water sources near Arusha region. Red dots correspond to water sources with fluoride levels higher than WHO recommendations. Blue dots are water sources with fluoride levels lower than 1.5 mg kg^{-1}. Reprint with permission from ACS Sens. 2021, 6, 1, 259–266 publication date: January 8, 2021, https://doi.org/10.1021/acssensors.0c02273 copyright © 2021 American Chemical Society.

between IQ and water fluoridation was recently reported, opening the possibility of pointing to fluoride as being a developmental neurotoxin [6].

Due to severe risks on human health, it is vital to study the long-term effects of fluorides in the population, have strict control on the fluoride intake, and develop techniques to provide reliable quantification of fluoride on drinking water.

The analytical methodologies for fluoride quantification range from electrochemical approaches to colorimetric methodologies, by using naked eye detection or by means of spectrophotometric measurements. The more reliable quantification methodologies performed in laboratories, require trained operators to perform the quantification and to accurately interpret the results. However, these instruments are often out of reach for the majority of the communities in developing countries.

In order to develop accessible, reliable, and sustainable fluoride quantification methodologies, it is important to understand the chemistry involved and how new technologies like 3D printing, low-cost electronics using Arduino, and the use of smartphones as interfaces can make a major contribution to the improvement of the user experience.

In this chapter, an overview of the traditional fluoride quantification methodologies and those emerging from the use of advanced materials like Metal–Organic Frameworks will be found. Also, the implementation of smartphones as user interfaces for analytical determinations will be discussed, prioritizing the easiness, fast response, and accessibility of the methodology.

In some cases, a compromise between the accuracy or the application range will be found, but always keep in mind the convenience of the final user and the democratization of science and tech.

2. Analytical methods for fluoride determination

2.1 Electrochemical methods

The fluoride-selective electrode is a measuring electrode whose potential depends on the concentration of fluoride ions (F^-) in the solution in which it is immersed. It serves as a sensor to determine the concentration of fluoride ions. This electrode must be immersed in the solution together with a separate or built-in reference electrode so that the voltage between the electrodes can be measured with a suitable measuring instrument—some devices also convert the voltage into a concentration. A fluoride electrode can be used in a fairly wide concentration range—typically from 10^{-6} to $0.1\,mol\,L^{-1}$. Therefore, the determination method with the fluoride electrode is the most important and most frequently used for the direct determination of fluoride in drinking water. The most important part of the fluoride-selective electrode is a membrane made of a solid fluoride ion conductor, mostly a single crystal of lanthanum fluoride LaF_3, which has been doped with europium ions, Eu^{+2}. This membrane does not measure the concentration, but the activity of the fluoride ions. In order to obtain reliable measured values even for samples with fluctuating ionic strength, The sample has to be conditioned before the measurement by adding a special buffer solution (TISAB, total ionic strength adjustment buffer). This also ensures that the pH value is not too high, as hydroxide ions can interfere with the measurement. TISAB also contains reagents that react with trivalent ions, like aluminum (Al^{+3}) and iron (Fe^{+3}), forming complexes and thus preventing them from binding fluoride and thus causing a wrong fluoride determination. Then, the voltage between the fluoride-selective electrode and a reference electrode is measured. It is given according to the Nernst equation, taking into account the single negative charge of the fluoride ion

$$E = E^0 - \frac{RT}{F} . \ln \alpha_{F^-} = E^0 - \frac{RT}{F} . \ln c_{F^-} - \frac{RT}{F} . \ln \gamma_{F^-} \tag{1}$$

where
E Electrode potential measured on the fluoride electrode against the reference electrode.
E^0 Electrode potential against the same reference and with $\alpha_{F^-} = 1$.
$R = 8.31447\,J\,K^{-1}\,mol^{-1}$.
T Absolute temperature in Kelvin: $273.15 + C^o$.
F Faraday constant: $96485.34\,C\,mol^{-1}$.
a_{F^-} Activity of fluoride anions.
c_{F^-} Concentration of fluoride anions.
With the addition of TISAB, the activity coefficients keep constant and the expression simplifies to:

$$E = E^{0'} - \frac{RT}{F} \ln c_{F^-} \tag{2}$$

with

$$E^{0'} = E^0 - \frac{RT}{F} \ln \gamma_{F^-} \tag{3}$$

At constant ionic strength, pH, and 25°C, the expression is reduced to

$$E = E^{0'} - 59.2 \, \mathrm{mV} c_{F^-} \tag{4}$$

2.2 Spectroscopic methods

Spectroscopic methods are based on the high affinity of fluorides to certain metals. A colored complex can exchange its ligands with fluorides and change the color of the solution. This change can be quantified using the Lambert–Beer law using spectro-photometric measurements. For this type of determination, it is necessary to quantify the attenuation of a light source passing through a medium, in this case, the solution containing the metal complex and the fluorides. The light from a light source of Irradiance P will pass through an *infinitesimally thin* layer of the sample dx. During the light absorption process, the irradianace P will decay its power in dP, this decay will be proportional to the concentration of colored complexes c, the probability of light absorption β, and the thickness of the section dx:

$$dP = -\beta.P.c \; dx \tag{5}$$

The negative sign in the expression indicates that P decreases while passing through the solution.
This expression can be rearranged to:

$$-\frac{dP}{P} = -\beta.c \; dx \Rightarrow -\int_{P_0}^{P} \frac{dP}{P} = \beta.c \int_{0}^{b} dx \tag{6}$$

If we integrate this expression with limits $P = P_0$ at $x = 0$ and $P = P$ at $x = b$.

$$-\ln P - (-\ln P_0) = \beta.c.b \Rightarrow \ln \frac{P_0}{P} = \beta.c.b \tag{7}$$

Changing the logarithm base, we obtain:

$$A = \log \frac{P}{P_0} = \frac{\beta}{\ln 10}.c.b = \varepsilon.c.b \Rightarrow A = \varepsilon.c.b \tag{8}$$

This is the linear relationship between concentration and Absorbance, A, where c is the concentration of the colored analyte, b the optical path, and ε a proportional factor.

As the reaction of fluorides with a metal complex causes a change in the color intensity and this change is proportional to the fluoride concentration, the fluoride concentration can be determined using the expression $A = \varepsilon.c.b$.

The use of spectrophotometric methods to determine fluorides has a long story due to the simplicity with respect to electrochemical methods, and the most relevant will be described herein.

2.2.1 Fe-SCN system

The $Fe(SCN)^{+2}$ complex has a characteristic strong red color while the fluoride analog is colorless. The disappearance of the red color in presence of fluoride can be
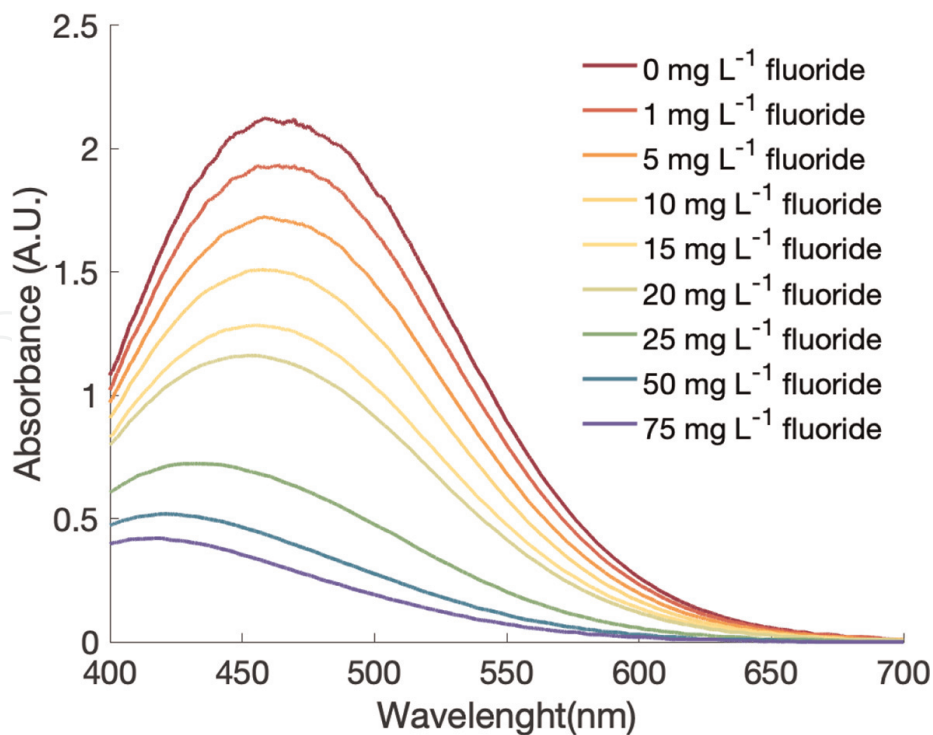
Figure 2.
Visible absorption spectra of FeSCN complex and the decrease of absorbance in presence of different concentrations of fluoride.

	FeSCN	FeF
$\log \beta_1$	2.09	5.5
$\log \beta_2$	3.30	9.7
$\log \beta_3$		12.7
$\log \beta_4$		14.9
$\log \beta_5$		15.4

Table 1.
Formation constants for Fe(III) complexes with thiocyanate and fluoride.

used for quantification purposes, and the changes in the UV–Vis spectra can be observed in **Figure 2**. The fluoride and thiocyanate complexes formation constant are shown in **Table 1**, where fluoride complexes are more favorable than thiocyanate ones and the equilibrium is displaced according to the Eq. (9).

$$\text{Fe(SCN)}_n^{3-n} + m \ \text{F}^- \leftrightarrow \text{FeF}_m^{3-m} + n \ \text{SCN}^- \tag{9}$$
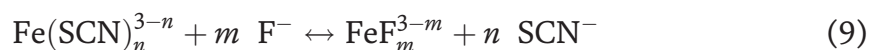
Even though this method was reported in 1933 for the first time [7], it was recently implemented in a portable sensor, which achieves the WHO limits in drinking water [4]. This methodology has the advantage of being low cost, with reagents easily found in every chemistry lab. Also, the construction of the test strips using cotton as substrate, allows controlling the amount of sample used, being reproducible and user friendly. The sample enters the reaction zone by capillarity within the highly hygroscopic substrate. The quantification can be performed in two ways: (1) using photographs that the user makes from the test strips. Then the image is analyzed by splitting

the signal in the Red, Green, and Blue channels (**Figure 3**). (2) using an Arduino-based device, which can be connected to a smartphone and the data is received, processed, visualized, and shared through an application [8]. Under the optimized conditions, the image analysis showed a linear range up to 15 mag L^{-1}, Relative
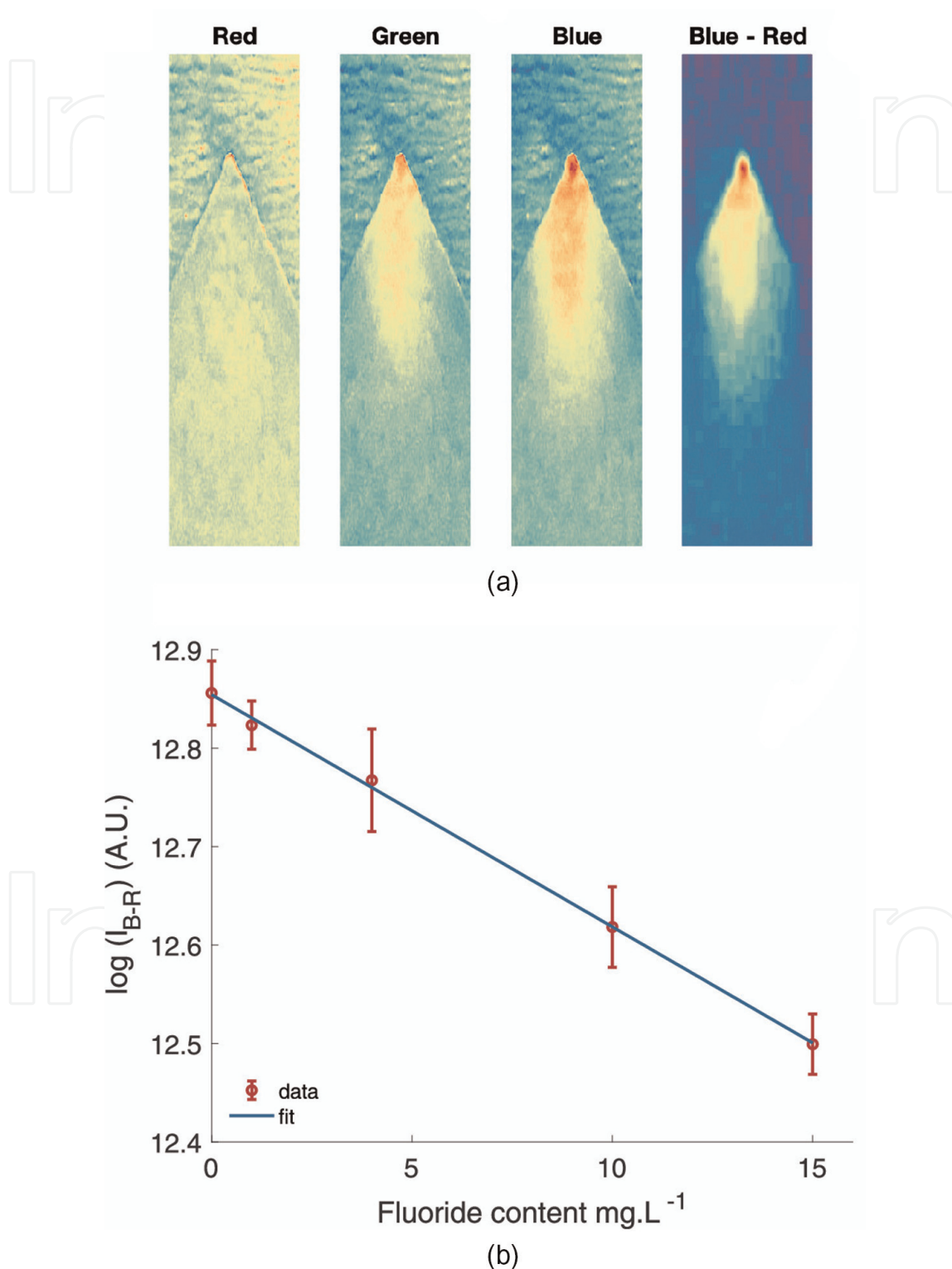

(a)

(b)

Figure 3.
(a) Images of the red, green, blue channels and the difference between blue and red components of the image. (b) Calibration curve obtained using "image analysis" quantification method using 20 μL of 0.33 mM Fe(III) in 0.4 M HClO$_4$ and 20 μL of 2.6 M SCN$^-$ in the test strip. Sample volume approx. 260 μL. reprinted with permission from ACS Sens. 2021, 6, 1, 259–266 publication date: January 8, 2021, https://doi.org/10.1021/acssensors.0c02273 copyright Â© 2021 American Chemical Society.

Standard Deviation or RSD% of 4.3%, and a Limit of Detection or LoD of 2.8 mg L^{-1}. On the other hand, the colorimetric Arduino-based analysis showed a linear range up to 8 mg L^{-1}, RSD of 5.1%, and LoD of 0.7 mg L^{-1}. Even though the LoD values are higher than other colorimetric methodologies, the Fe-SCN methodology showed excellent recovery % even in the presence of other common anions and cations at higher concentrations than fluoride. Therefore, it is a simple, affordable yet appropriate methodology for the water quality assessment on areas where the fluoride concentration is high (e.g. United Republic of Tanzania) (**Figure 4**).
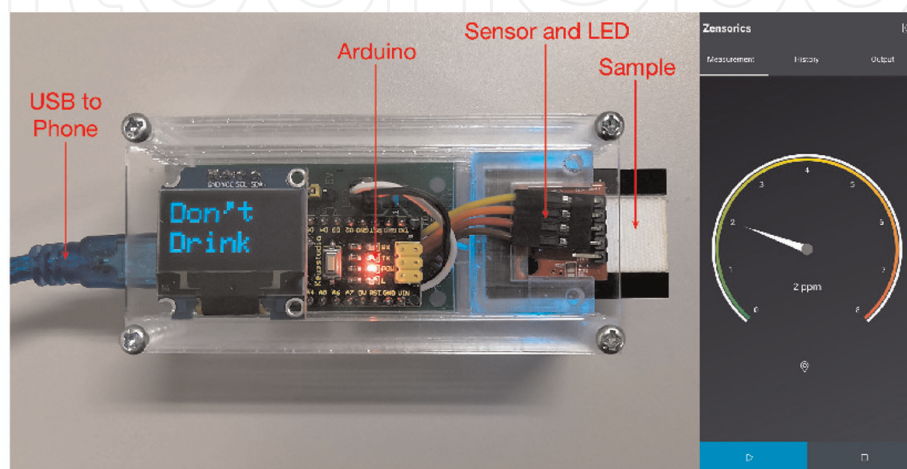
(a)
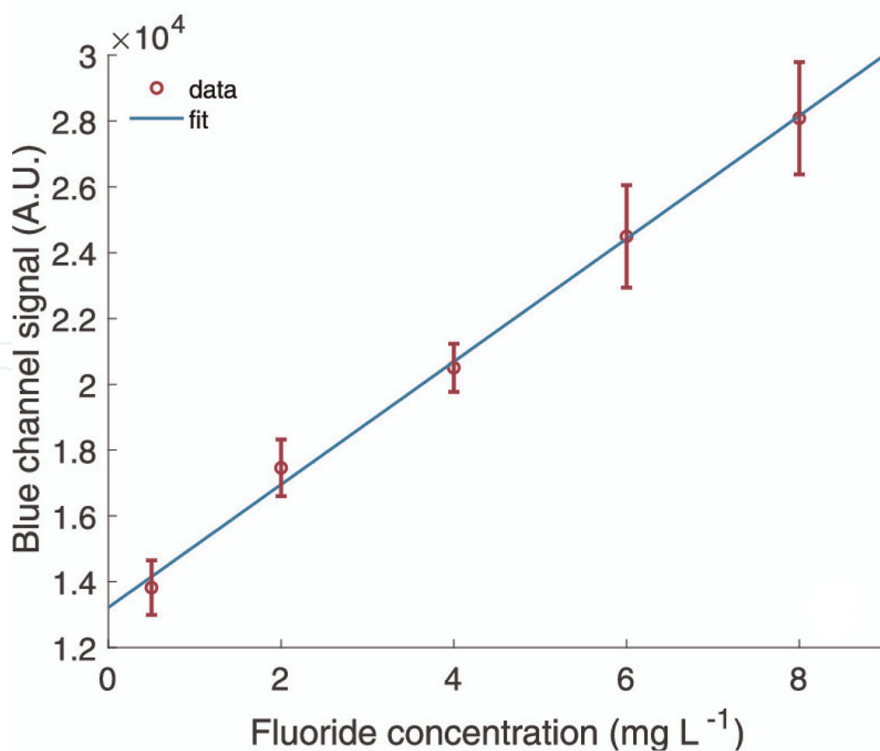
(b)

Figure 4.
(a) Photograph of the Arduino portable device for color quantification and the app developed for the visualization and data sharing (b) calibration curve obtained with the Arduino-based device. Adapted with permission from ACS Sens. 2021, 6, 1, 259–266 publication date: January 8, 2021, https://doi.org/10.1021/acssensors.0c02273 copyright © 2021 American Chemical Society.

2.2.2 Alizarin complexes

One of the most used and old methodologies for fluoride detection and quantification methodologies are those using Alizarin complexone (AC)(2-[carboxymethyl-[(3,4-dihydroxy-9,10-dioxoanthracen-2-yl)methyl]amino]acetic acid). The complex of Ce^{+3} AC in acetonitrile media gives purple complexes and the absorbance changes with fluoride can be measured at 617 nm [9]. The standardized methodology using AC accepted by the Environmental Protection Agency (USA) [10], requires the fluoride distillation from the sample prior to the measurement, increasing the probability of error due to sample manipulation and increasing the operational difficulty.

Another useful method for fluoride determination is the Zr-Alizarin S red complex. In this case, Alizarin S red or simply Alizarin (**Figure 5**) shows a yellow color in the free form and changes to red-purple complex in presence of Zr. The quantification of fluoride can be performed at 520 nm measuring the decrease of the Alizarin-Zr complex or at 425 nm, measuring the free Alizarin form freed when fluoride is present (**Figure 6**).
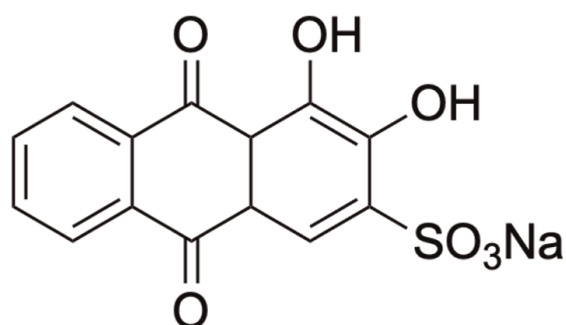

Figure 5.
Structure of 3,4-Dihydroxy-9,10-dioxo-9,10-dihydroanthracene-2-sulfonic acid, also known as alizarin S red.
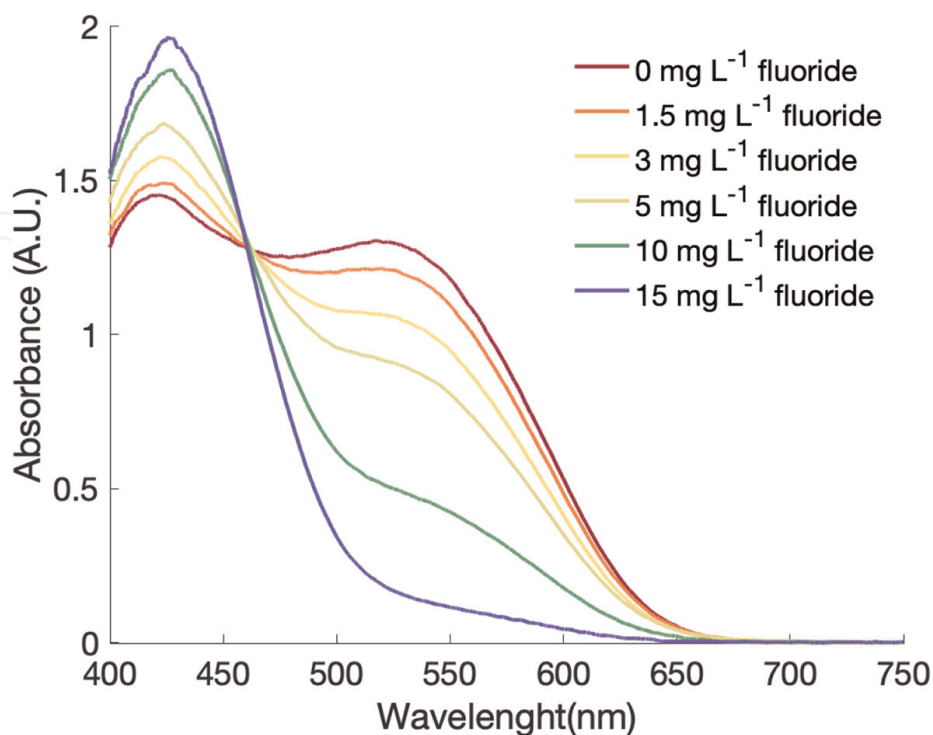

Figure 6.
Visible absorption spectra of Zr-alizarin S red complex and the decrease of absorbance in presence of different concentrations of fluoride.

2.2.3 Zr-SPADNS system

Nowadays, the accepted standardized methodology is the ion-selective methodology described above [11], but for practical reasons, many qualitative and semi-quantitative methodologies based on the colorimetric reaction of 2-(parasulfo-phenylazo)-1,8-dihydroxy-3,6-naphthalene-disulfonate (SPANDS, see **Figure 7**) and Zr(II) with fluorides are found [12] (see **Figure 8**). The Environmental Protection Agency uses the Zr-SPANDS methodology as their standardized methodology [13]. Commercial test strips, online methodologies [14, 15], and on-site test kits are available elsewhere showing good reproducibilities and moderately narrow linear ranges that limit their application to waters where the fluoride content is below 5 mg L^{-1}.
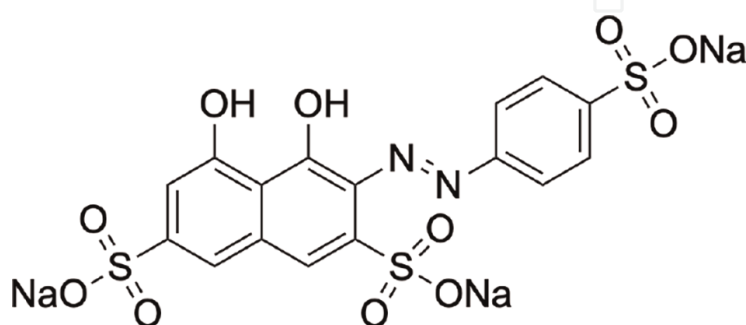

Figure 7.
2-(4-Sulfophenylazo)-1,8-dihydroxy-3,6-naphthalenedisulfonic acid trisodium salt, also known as SPADNS.
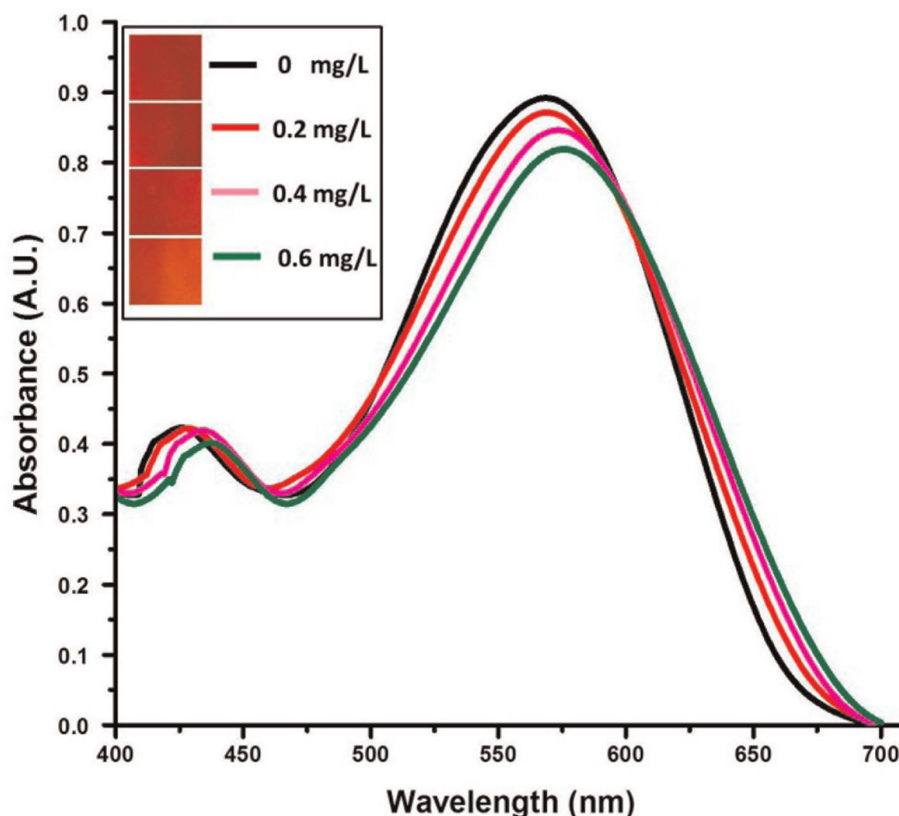

Figure 8.
Absorption spectrum of zirconium–SPADNS dye mixed with water sample containing fluoride ion at different concentrations; the inset shows the photo images of the corresponding samples. Reprinted with permission from anal. Chem. 2017, 89, 1, 767–775 publication date: December 1, 2016, https://doi.org/10.1021/acs.analche m.6b03424 copyright © 2016 American Chemical Society.

2.3 Chemosensors

As previously mentioned, the determination of fluorides in-situ is a powerful tool to provide information about the water quality in rural communities. Even though the use of ion-selective electrodes in field measurements, the simplification of spectroscopic instrumentation has far lower costs. To simplify a spectrometer is only needed to have a monochromatic light source with respect to the absorption band of the complex, a light intensity detector, and an electronic setup to read the detector output. Nowadays, this setup can be constructed using an LED as a light source, a photodiode, and a single-board microcontroller, e.g. Arduino. Also, this detector can be integrated into smartphones, providing extended capabilities.

Hussain et al. [16] reported the integration of an optical system to a smartphone (Sony Xperia E3) using Zr-SPADNS as a chemical system, ambient light sensor as a light detector, the flashlight as light source, fiber optics, and the smartphone for data collection, see **Figure 9** for optical set-up and smartphone app. Levin et al. [17] followed a similar path using zirconium xylenol orange reagent as a chemical system and using three different smartphones to test the device. Mukherjee et al. [18] used core-shell nanoparticles (near-cubic ceria@zirconia nanocages) and the same chemoresponsive dye (xylenol orange) attached to a smartphone, obtaining a linear range up to 5 mg L^{-1} and LoD = 0.1 mg L^{-1}. Otal et al. [4] use of the Fe-SNC system but instead of using the reagents in solution, the chemical were impregnated into cotton, which reduces the chemicals manipulation and provides strict control over the volume of the sample. They reported a linear range up to 8 mg L^{-1} and a LoD of 0.7 mg L^{-1}.

2.3.1 MOFs based sensors

Metal–organic Frameworks (MOFs) are a family of coordination polymers with a high surface area that can be used for water sensors among other applications. A MOF has three main points of interest:

An organic ligand, **Figure 10**, is a rigid organic molecule that is coordinated to metals and/or metallic centers. The most common coordination moiety is a carboxylate, but every moiety previously used in coordination compounds can be used here also. The ligand is the organic part and manages the isoreticular chemistry, which means that keeping unchanged the metal and the coordination moieties but changing the length of organic chain among the coordination points, the connectivity in the MOF keeps constant but the cell parameters can be expanded. An example of this is a series from UiO-66 to UiO-68, which systematically includes terephtalic acid (UiO-66), 4,4′-biphenyldicarboxylic acid (UiO-67), and p-Terphenyl-4,4″-dicarboxylic acid (UiO-68) (see **Figure 10**). Another remark about the ligand is the possibility to perform post-synthetic modification (PSM), which allows applying all the organic chemistry reactions on the synthons of these molecules (e.g. amino groups, see **Figure 10**). This toolbox is well known for many decades [19] and can be used to enhance gas storage and separation [20] and to improve photocatalytic performance [21].

A metal center, **Figure 11**. The metal center, also known as *Secondary Building Unit* (SBU), determines the topology of the MOF and also has rich chemistry due to the possibility to form *open metal sites*, which are uncoordinated metallic centers due to dangling ligands. Also the chance to include different metals in the same SBU or change the oxidation state make them an active field of research. The nature of these
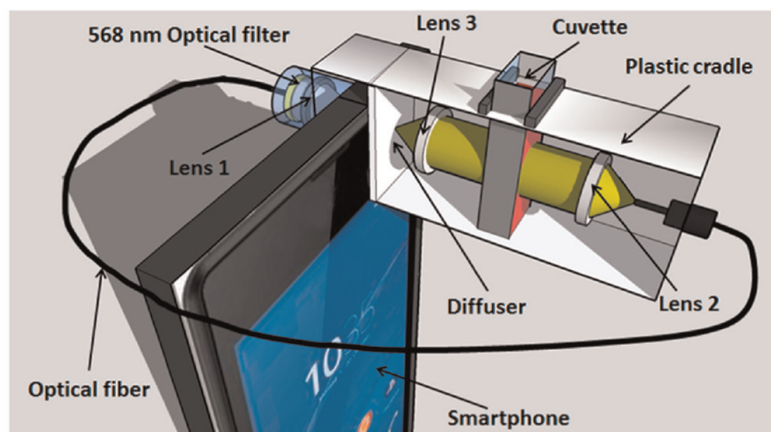
(a)

(b)
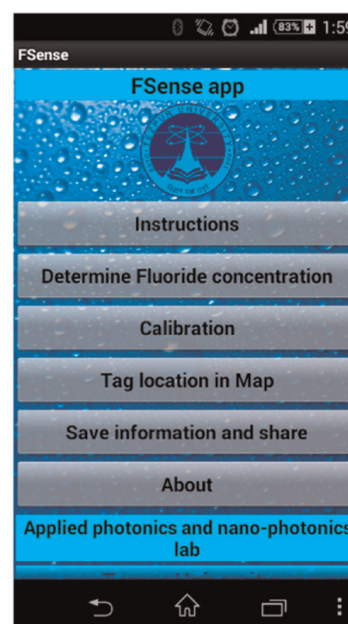
(c)

Figure 9.
(a) Schematic of the smartphone-based fluoride sensor; (b) photograph of the designed sensor; and (c) a screenshot image of the developed "FSense" application for the present sensor. Reprinted with permission from anal. Chem. 2017, 89, 1, 767–775 publication date: December 1, 2016, https://doi.org/10.1021/acs.analchem.6b03424 copyright © 2016 American Chemical Society.
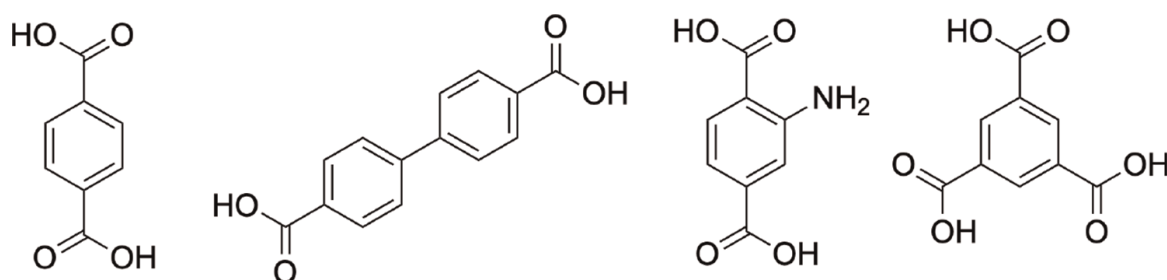

Figure 10.
Common ligands used in MOFs. From left to right: Benzene-1,4-dicarboxylic acid (terephthalic acid or BDC), Biphenyl-4,4'-dicarboxylic acid (BPDC), 2-aminobenzene-1,4-dicarboxylic acid (2-Aminoterephthalic acid), and Benzene-1,3,5-tricarboxylic acid (Trimesic acid or BTC).
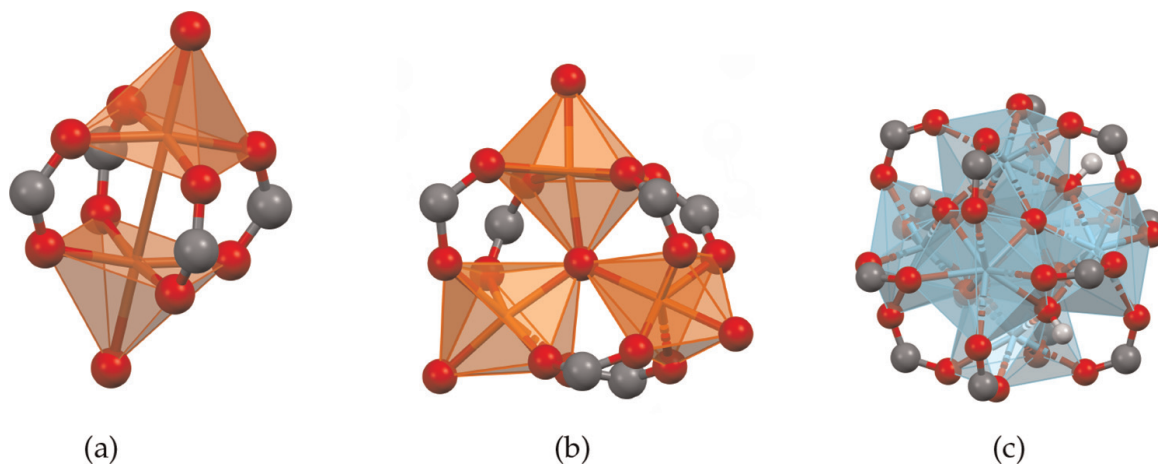
Figure 11.
Secondary building units (SBU) of selected MOFs.

centers can be from simple metal to metal–metal ligands in MOF-199 and to metal-oxo cluster like in UiO-66, see 11.

A pore, **Figure 12**. The pore is the natural consequence of the implementation of rigid ligands in a coordination polymer. The rigid ligands will keep the distance between the SBU and create a void in the center of the MOF lattice.

MOF fluoride sensors are based on the interaction of the fluorides with the SBU. This interaction is based on the affinity of the fluorides with the metal in the SBU. The metals which exhibit a strong interaction with fluorides are Al, Fe, Zr, and lanthanides. The interaction mechanism is related to the formation of a complex ion in the case of Al, Fe, and Zr, while lanthanides can form the respective fluorides, which are insoluble.
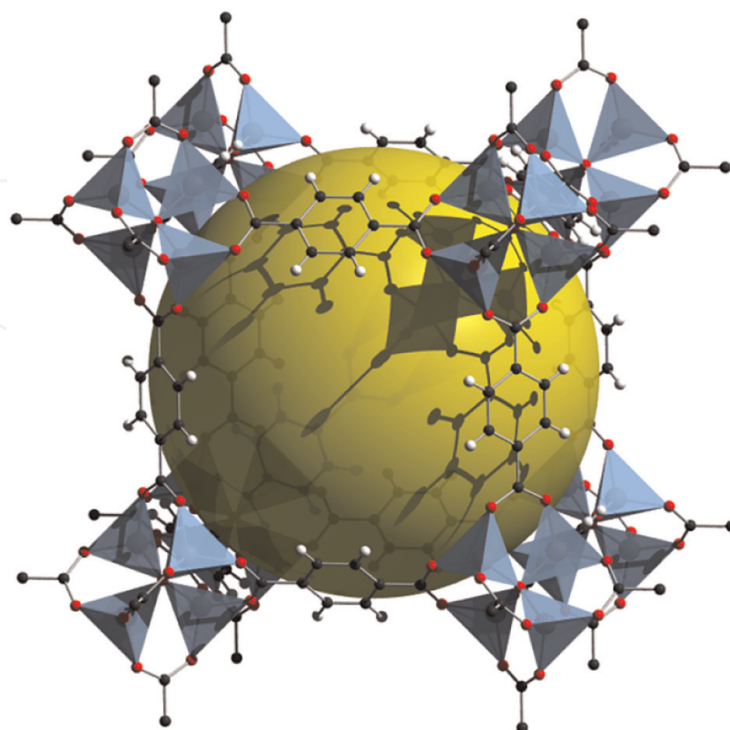

Figure 12.
Pore in MOF-5, blue tetrahedral are the Zn atoms coordinated by carboxylates and the yellow sphere represents the pore volume.

13

Chen and coworkers [22] used their Tb-BTC (BTC = Benzenetricarboxylates) for the fluoride detection in organic solvents like methanol and dimethylformamide. The authors found an increase of the luminescence in the presence of fluoride, with a sensing mechanism given by the confinement of the anion on the MOF's micropores, and the interaction of F$^-$ through hydrogen bond with the solvent molecules. The intrinsic luminescence of Tb^{+3} ions is enhanced as the quenching effect of O–H bonds from the solvent is decreased.

Honjo et al. [23] used the same MOF but grown inside a liposome. And contrary to Chen, they found a decrease in the luminescence of Tb-BTC in the presence of fluoride in an aqueous buffered media (HEPES 20 mM). They found an increase in the sensitivity of these confined nanocrystals when compared with the bulk MOFs due to the enhanced dissolution of the MOF towards the formation of Tb-F non-fluorescent species. In this case, the linear range found was up to 2 mg L^{-1}.

Otal and co-workers [24] developed a portable textile-based sensor using Tb-BTC@cotton, improving the applicability of the sensor to on-site measurements of natural waters. The authors demonstrated the TbF$_3$ formation using synchrotron X-ray absorption fine structure measurements and proposed a 3-staged mechanism of interaction between fluorides and the luminescent MOF according to the fluoride concentration. For a given amount of solid, at low fluoride concentrations, there is an increase of luminescence with the anion concentration (ligand exchange region). These results are in agreement with the ones reported by Chen et al. [22] who also obtained an increase of the MOF luminescence with fluoride concentration. Then a "saturation" zone is observed, where the increase of fluoride concentration does not modify the luminescence intensity of the system. Finally, a "Dissolution" region appears, where the emission of the MOF decreases due to the formation of TbF$_3$. The cotton test-strips and the Arduino-based sensor allowed to obtain an overall low cost and easy to handle fluoride quantification system, with an extended linear range of up to 10 mg L^{-1} of fluoride, with a limit of detection of 0.8 mg L^{-1} (**Figure 13**).

Hingerholzinger and co-workers [25] used NH$_2$-MIL-101(Al) and fluorescein 5(6)-isothiocyanate molecules confined in the MOFs micropores. In the presence of fluorides, the MOFs dissolved releasing the dye to the media and thus, increasing the luminescence of the solution. The authors reported a linear range for fluoride of 15–1500 μg L^{-1} with a high selectivity towards the analyte, even in the presence of concomitant ions like Cl$^-$, Br$^-$, nitrates, carbonates, sulfates, and acetates. Another encapsulation of a fluorescent dye, in this case, 2′,7′-dichlorofluorescein, into the same Al-based MOF was reported by Sun et al. [26].

Zirconium-based MOFs like UiO-66 and related MOFs are highly stable in water, have high porosity, chemical, and physical stability, and a great versatility via post-synthetic modifications through the linker. These MOFs are built with Zr$_6$O$_4$(OH)$_4$ metallic centers and 1,4-Benzenedicarboxylates (BDC) as organic ligands, but they can be changed by NH$_2$-BDC or other functional groups.

Zhu and co-workers [27] used NH$_2$-UiO-66 for fluoride sensing and quantification in waters. The mechanism proposed by the authors relies on the hydrogen bond formation between the fluoride and the amino groups of the linkers. The withdrawal of electronic density away from the metallic center produces an increase in the luminescence, with a linear range up to 50 mg L^{-1} and a LoD of 0.229 mg L^{-1} of fluoride, even in the presence of common concomitants.

Also, UiO-66 MOFs were used as host frameworks for fluorescent guests within their structure. Inorganic guests like Tb^{+3} were tested for fluoride detection by
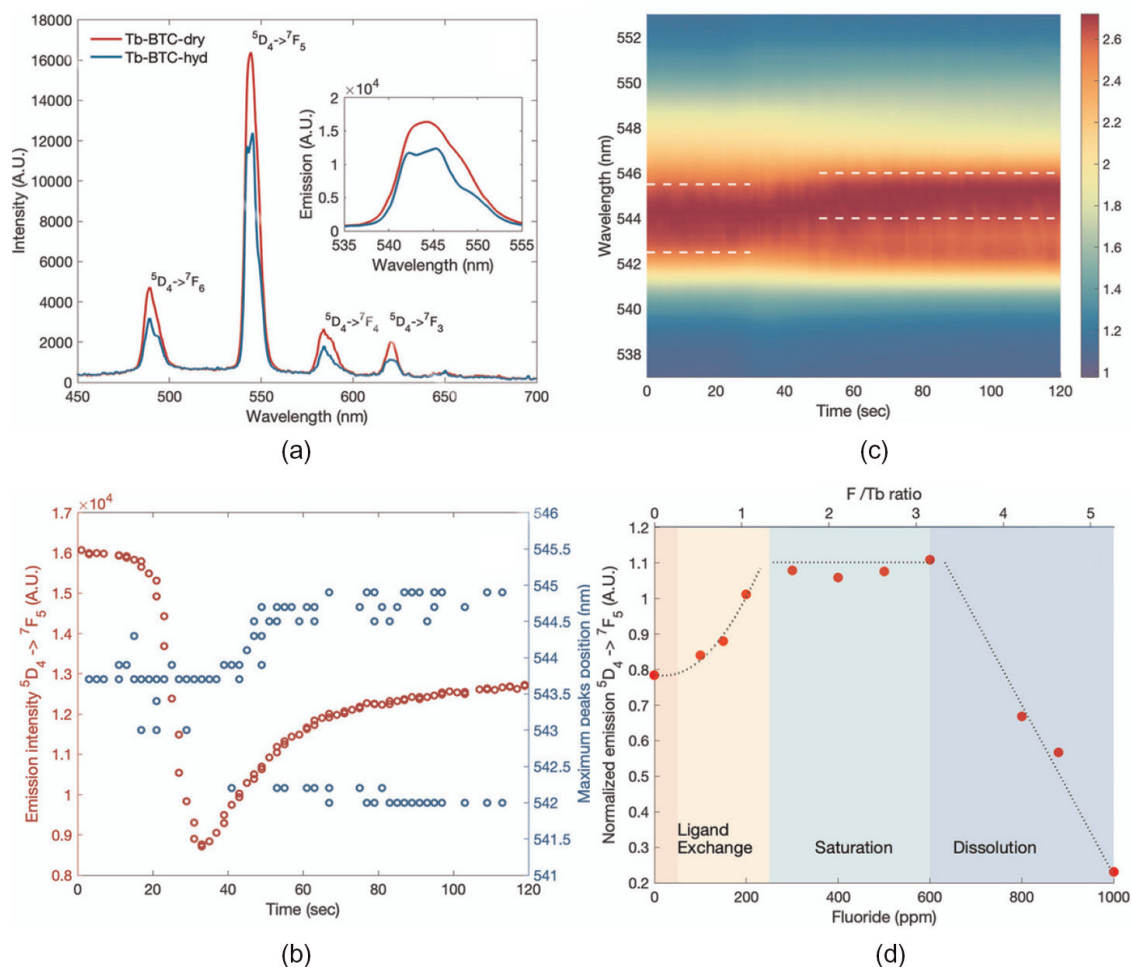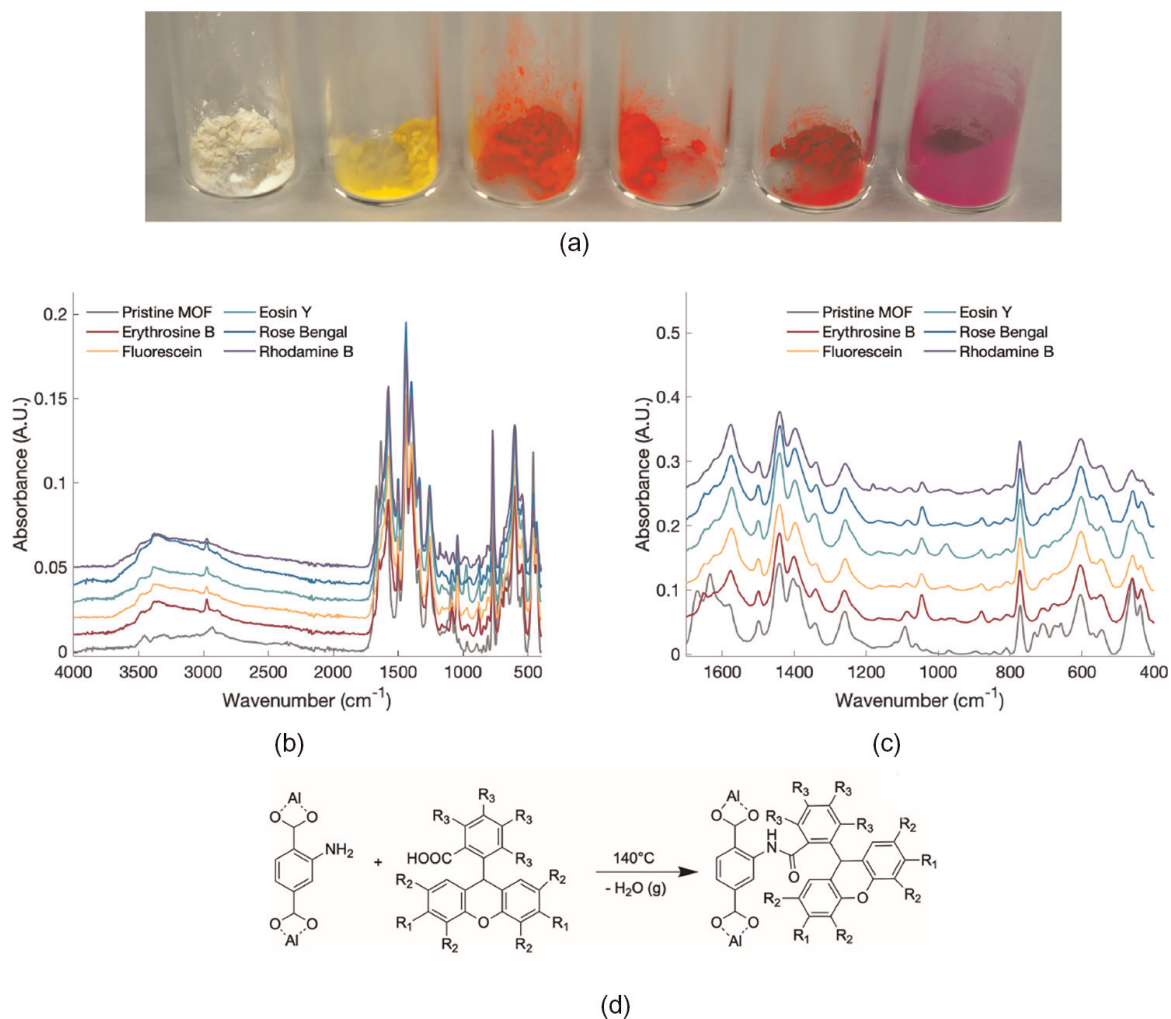
Figure 13.
(a)Emission spectra of TbBTC modified cotton before and after water exposure. (b) Intensity and maximum signal position sample are in contact with water. (c) Normalized intensity in function of time when the sample is in contact with water. (d) Intensity in function of F to Tb ratios. Regions of the proposed mechanism. Adapted with permission from [24].

incorporating open metal sites on the MOF through the partial substitution of BDC linker (**Figure 12**) with isopthalates [28]. The uncoordinated carboxy groups incorporate Tb(III) via post-synthesis which conferred a strong luminescence to the final solid. The MOFs were tested for fluoride detection, which enhanced the luminescence of the MOF and other anions like Cl^-, Br, NO_3^-, CO_3^{-2}, HCO_3^-, SiO_3^{-3}, SO_4^{-2}, and PO_4^{-3} produced a slight decrease of luminescence, and I^-, S^{-2}, and NO_2^- gave a total quenching of the MOF. The linear range was up to 40 mg L^{-1} and a LoD of 0.35 mg L^{-1}.

On the other hand, organic fluorescent guests (like fluorescein sodium) were used on UiO-66 MOFs structure [29]. The dissolution of the MOF and thus, the release of the fluorescent probe was proposed as a sensing mechanism, with a linear range up to 7.6 mg L^{-1} and a LoD of 0.08 mg L^{-1}.
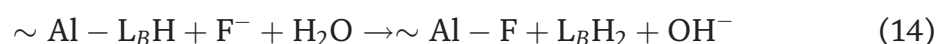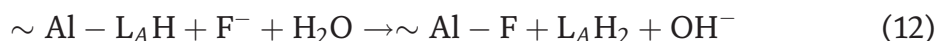
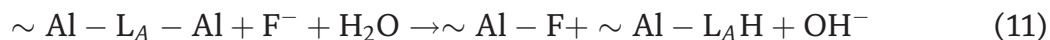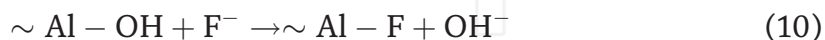Recently our group developed a simple post-functionalization procedure for Al-BDC MOFs through a thermal treatment [30] opening the possibilities towards new MOFs for fluoride sensing (**Figure 14**).

Several xanthene dyes were used as modifiers (i.e. Fluorescein, Rhodamine B, Eosin Y, Erythrosine B, and Rose Bengal) and the dissolution of the MOF in presence of fluoride and the release of the dye to the solution was measured.

(a)

(b)

(c)

(d)

Figure 14.
(*a*) *Photograph of the modified MOF, from left to right: Al-BDC-NH₂, Fluorescein, Eosin Y, Erythrosine B, Rose Bengal and rhodamine B. FTIR spectra from the modified and unmodified MOFs, (**b**) complete spectra and (**c**) carboxylate region. Adapted with permission from [30]. Adapted from [30] (**d**) proposed synthetic pathway for the formation of the amide. For fluorescein: $R_1 = -OH$, $R_2 = R_3 = -H$, rhodamine B: $R_1 = -N(et)_2$, $R_2 = R_3 = -H$, rose bengal: $R_1 = -OH$, $R_2 = -I$, $R_3 = -Cl$, eosin Y: $R_1 = -OH$, $R_2 = -Br$, $R_3 = -H$, and erythrosine B: $R_1 = -OH$, $R_2 = -I$, $R_3 = -H$. Adapted with permission from [30].*

Excellent recovery% was obtained even in the presence of common concomitants in waters, with a sensing mechanism governed by ligand exchange and dye release to the aqueous media (Eqs. (10)–(14)).

$$\sim Al - OH + F^- \rightarrow \sim Al - F + OH^- \tag{10}$$

$$\sim Al - L_A - Al + F^- + H_2O \rightarrow \sim Al - F + \sim Al - L_AH + OH^- \tag{11}$$

$$\sim Al - L_AH + F^- + H_2O \rightarrow \sim Al - F + L_AH_2 + OH^- \tag{12}$$

$$\sim Al - L_B - Al \sim + F^- + H_2O \rightarrow \sim Al - F + \sim Al - L_BH^+ OH^- \tag{13}$$

$$\sim Al - L_BH + F^- + H_2O \rightarrow \sim Al - F + L_BH_2 + OH^- \tag{14}$$

3. Future perspectives

The chemosensors and MOF-based sensors for fluoride showcased in this chapter showed varied opportunities for naked-eye or instrumental-based colorimetric and fluorometric detection.

However, most of the sensors showed limited linear ranges and relatively high LoD values. According to current international regulations, these sensors could be of interest for their applications in rural areas and for low-cost devices. But if the levels of suggested upper limits of fluorides drop to lower values than 1.5 mg L^{-1}, then the sensitivity of these sensors should be improved. The application of Metal–Organic Frameworks for fluoride sensing is a growing area of research and it is expected the development of new materials with lower cost and better performance in the next years.

Current commercial test kits are semi-quantitative or qualitative methodologies and still rely on the human eye for reading and interpretation. They also need the reagents handling, with short shelf lives that might lead to errors and biased results that could affect human health at different levels. Therefore, the implementation of mobile phones as user-friendly devices for the quantification, monitoring, and data sharing platforms might allow the extended reach of new materials and technologies to the final users, giving accurate unbiased results, at low costs and easy sample handling.

Appendix A: common quality parameters for the analytical methodologies

Linear range Is the analyte concentration range where the response of the analytical methodology is linear and proportional to the amount of the target analyte.

Limit of Detection Is the amount of analyte giving a *significative different* signal from the blank sample. With significative differences, the statistical meaning is considered.

$$Y_{\text{LoD}} = Y_{\text{blank}} + 3S \tag{15}$$

where Y_{LoD} is the signal of the minimum amount of analyte, Y_{blank} is the signal given by the blank sample and then, the LoD from the calibration curve can be calculated simply by

$$\text{LoD} = 3S/m \tag{16}$$

being m, the sensitivity of the analytical methodology or the slope of the linear regression.

Accuracy Indicates how close to the *real value* is the results obtained with the analytical methodology. The evaluation of the method accuracy can be performed by using a certificate material, spiking a real sample, comparing the developed methodology with other analytical techniques, etc.

Relative Standard Deviation Gives a measurement of the precision of the methodology, especially useful when it has to be compared with other analytical methodologies available for the same analyte. It can be calculated by

$$\text{RSD} = 100 * S/\overline{x} \tag{17}$$

where $\overline{x}$ is the mean value of N replicates.

Author details

Eugenio Hernan Otal[1†], Manuela Leticia Kim[1†] and Mutsumi Kimura[1,2,3*]

1 Faculty of Textile Science and Technology, Department of Chemistry and Materials, Shinshu University, Ueda, Nagano, Japan

2 COI Aqua-Innovation Center, Shinshu University, Ueda, Nagano, Japan

3 Research Initiative for Supra-Materials, Shinshu University, Ueda, Nagano, Japan

*Address all correspondence to: mkimura@shinshu-u.ac.jp

† These authors contributed equally.

IntechOpen

References

[1] Gooch BF. Community water fluoridation—One of the 10 greatest public health achievements of the 20th century. Blogs|CDC. 2015;**130**(4): 296-298. Available from: https://blogs. cdc.gov/pcd/2015/04/23/community-wa ter-fluoridation-one-of-the-10-greatest- public-health-achievements-of-the- 20th-century/

[2] Organization WH. Guidelines for Drinking-water Quality. Geneva Switzerland: World Health Organization; 1993

[3] Yeung CA. A systematic review of the efficacy and safety of fluoridation. Evidence-Based Dentistry. 2008;**9**(2): 39-43. Available from: https://www.na ture.com/articles/6400578

[4] Otal EH, Kim ML, Dietrich S, Takada R, Nakaya S, Kimura M. Open- source portable device for the determination of fluoride in drinking water. ACS Sensors. American Chemical Society. 2021;**6**(1):259-266. DOI: 10.1021/acssensors.0c02273

[5] Gravitz L. The fluoride wars rage on. Nature. 2021. DOI: 10.1038/d41586-021- 02924-6. Available from: https://www. nature.com/articles/d41586-021-02924-6

[6] Grandjean P, Hu H, Till C, Green R, Bashash M, Flora D, et al. A benchmark dose analysis for maternal pregnancy urine-fluoride and IQ in children. medRxiv. 2020;**10**(31):20221374. Available from: https://www.ncbi.nlm. nih.gov/pmc/articles/PMC7654913/

[7] Foster MD. Colorimetric determination of fluoride in water using ferric chloride. Industrial & Engineering Chemistry Analytical Edition. American Chemical Society. 1933;**5**(4):234-236. DOI: 10.1021/ac50084a005

[8] Dietrich S. Zensorics App. Available from: https://hello.fridie.de/zensorics- app/

[9] Yamamura SS, Wade MA, Sikes JH. Direct Spectrophotometric Fluoride Determination. Analytical Chemistry. American Chemical Society. 1962; **34**(10):1308-1312. DOI: 10.1021/ ac60190a033

[10] EPA. Methods for Chemical Analysis of Water and Wastes. Cincinnati, OH: Environmental Protection Agency; 1979. Available from: https://www.osti.gov/b iblio/6259902-methods-chemical-ana lysis-water-wastes

[11] ASTM International. ASTM D1179-16—standard test methods for fluoride ion in water. Engineering; **360**:2-4. Available from: https:// standards.globalspec.com/std/3861620/ astm-d1179-16

[12] Marier JR, Rose D. The fluoride content of some foods and beverages–a brief survey using a modified Zr- SPADNS method. Journal of Food Science. 1966;**31**(6):941-946. DOI: 10.1111/j.1365-2621.1966.tb03273.x. Available from: https://onlinelibrary. wiley.com/doi/abs/10.1111/ j.1365-2621.1966.tb03273.x

[13] US EPA O. Method 13A—Total Fluoride—SPADNS Zirconium Lake [Other Policies and Guidance]. 2016. Available from: https://www.epa.gov/e mc/method-13a-total-fluoride-spad ns-zirconium-lake

[14] Arancibia JA, Rullo A, Olivieri AC, Nezio SD, Pistonesi M, Lista A, et al. Fast spectrophotometric determination of fluoride in ground waters by flow injection using partial least-squares

calibration. Analytica Chimica Acta. 2004;**512**(1):157-163. Available from: https://www.sciencedirect.com/science/article/pii/S0003267004002168

[15] Marques TL, Coelho NMM. Proposed flow system for spectrophotometric determination of fluoride in natural waters. Talanta. 2013;**105**:69-74. Available from: https://www.sciencedirect.com/science/article/pii/S0039914012010247

[16] Hussain I, Ahamad KU, Nath P. Low-cost, robust, and field portable smartphone platform photometric sensor for fluoride level detection in drinking water. Analytical Chemistry. American Chemical Society. 2017;**89**(1):767-775. DOI: 10.1021/acs.analchem.6b03424

[17] Levin S, Krishnan S, Rajkumar S, Halery N, Balkunde P. Monitoring of fluoride in water samples using a smartphone. The Science of the Total Environment. 2016;**551-552**:101-107

[18] Mukherjee S, Shah M, Chaudhari K, Jana A, Sudhakar C, Srikrishnarka P, et al. Smartphone-based fluoride-specific sensor for rapid and affordable colorimetric detection and precise quantification at sub-ppm levels for field applications. ACS Omega. American Chemical Society. 2020;**5**(39):25253-25263. DOI: 10.1021/acsomega.0c03465

[19] Kalaj M, Cohen SM. Postsynthetic modification: An enabling technology for the advancement of metal–organic frameworks. ACS Central Science. American Chemical Society. 2020;**6**(7):1046-1057. DOI: 10.1021/acscentsci.0c00690

[20] Li B, Wen HM, Zhou W, Chen B. Porous metal–organic frameworks for gas storage and separation: What, how,
and why? The Journal of Physical Chemistry Letters. American Chemical Society. 2014;**5**(20):3468-3479. DOI: 10.1021/jz501586e

[21] Otal EH, Kim ML, Calvo ME, Karvonen L, Fabregas IO, Sierra CA, et al. A panchromatic modification of the light absorption spectra of metal–organic frameworks. Chemical Communications. Royal Society of Chemistry. 2016;**52**(40):6665-6668. Available from: https://pubs.rsc.org/en/content/articlelanding/2016/cc/c6cc02319c

[22] Chen B, Wang L, Zapata F, Qian G, Lobkovsky EB. A luminescent microporous metal–organic framework for the recognition and sensing of anions. Journal of the American Chemical Society. 2008;**130**(21):6718-6719. DOI: 10.1021/ja802035e

[23] Honjo M, Koshiyama T, Fukunaga Y, Tsuji Y, Tanaka M, Ohba M. Sensing of fluoride ions in aqueous media using a luminescent coordination polymer and liposome composite. Dalton Transactions. The Royal Society of Chemistry. 2017;**46**(22):7141-7144. Available from: https://pubs.rsc.org/en/content/articlelanding/2017/dt/c7dt01071k

[24] Otal EH, Tanaka H, Kim ML, Hinestroza JP, Kimura M. The long and bright path of a lanthanide MOF: From basics towards the application. Chemistry—A European Journal. 2021;**27**(26):7376-7382. DOI: 10.1002/chem.202005222 Available from: https://onlinelibrary.wiley.com/doi/abs/10.1002/chem.202005222

[25] Hinterholzinger FM, Rühle B, Wuttke S, Karaghiosoff K, Bein T. Highly sensitive and selective fluoride detection in water through fluorophore release from a metal-organic framework.

Scientific Reports. 2013;**3**(1):2562. Available from: https://www.nature.com/articles/srep02562

[26] Sun Y, Xu X, Zhao Y, Tan H, Li Y, Du J. Luminescent metal organic frameworks–based chemiluminescence resonance energy transfer platform for turn–on detection of fluoride ion. Talanta. 2020;**209**:120582. Available from: https://www.sciencedirect.com/science/article/pii/S0039914019312159

[27] Zhu H, Huang J, Zhou Q, Lv Z, Li C, Hu G. Enhanced luminescence of NH2-UiO-66 for selectively sensing fluoride anion in water medium. Journal of Luminescence. 2019;**208**:67-74. Available from: https://www.sciencedirect.com/science/article/pii/S0022231318315436

[28] Zheng HY, Lian X, Qin SJ, Yan B. Novel "turn-on" fluorescent probe for highly selectively sensing fluoride in aqueous solution based on Tb3+-functionalized metal–organic frameworks. ACS Omega. American Chemical Society. 2018;**3**(10): 12513-12519. DOI: 10.1021/acsomega.8b02134

[29] Zhao X, Wang Y, Hao X, Liu W. Fluorescent molecule incorporated metal-organic framework for fluoride sensing in aqueous solution. Applied Surface Science. 2017;**402**:129-135. Available from: https://www.sciencedirect.com/science/article/pii/S0169433217300764

[30] Otal EH, Kim ML, Hattori Y, Kitazawa Y, Hinestroza JP, Kimura M. Versatile covalent postsynthetic modification of metal organic frameworks via thermal condensation for fluoride sensing in waters. Bioengineering. 2021;**8**(12):196. Available from: https://www.mdpi.com/2306-5354/8/12/196